Content-Aware Cognitive Interference Control for Urban IoT Systems

Sabur Baidya and Marco Levorato
The Donald Bren School of Information and Computer Science, UC Irvine, CA, US
e-mail: {sbaidya, levorato}@uci.edu

***Abstract*—A novel cognitive interference control framework for heterogeneous local access networks supporting computing and data processing in Urban Internet of Things (IoT) systems is presented. The notion of cognitive content-aware interference control is introduced, where the transmission pattern of cognitive nodes is dynamically adapted to the state of "protected" IoT data streams. The state describes the performance degradation that interference would cause to algorithms processing the data if the cognitive nodes would chose to transmit in the corresponding time period. The framework is instantiated for a case-study scenario where Device-to-Device and Long-Term Evolution communications coexist on the same channel resource. A city-monitoring application is considered, where the state captures the type of frames within a multimedia video stream processed at the edge of the network to detect and track objects. Numerical results show that the proposed cognitive transmission strategy enables a significant throughput increase of local D2D communications for a target accuracy of the monitoring application.**

***Index Terms*—Device-to-Device Communications, LTE, Urban IoT, Video Streaming, Spectrum Sharing**

I. Introduction

The Internet of Things (IoT) is a recent communication paradigm that enables the interconnection and interoperation of everyday life objects, equipped with transceivers for digital communication and suitable protocol stacks [2]. An emerging trend proposes the application of the IoT paradigm to the urban environment [3,4], that is, the Urban IoT, which integrates city-wide sensing, communication and processing resources to improve the efficiency of public services.

We contend that the cognitive network paradigm [5,6] can play an important role in the design of networking technologies capable of supporting communications and computations in the complex Urban IoT scenario. One of the main challenges arises from the heterogeneity of the technologies supporting communications at different geographical scales, which often coexist on, and compete for, a shared channel resource. Importantly, in some application scenarios, communications supporting Urban IoT systems utilize the same frequency bands used by traditional wireless services. There is, then, a strong need for technological solutions facilitating the coexistence of heterogeneous data streams, especially for those applications where algorithms processing data streams in real-time may impose stringent and short term Quality of Service (QoS) requirements to the network.

In this paper, we propose a new framework, where cognitive techniques are used to control the interference generated by mutually interfering data streams, some of which may transport information critical to accomplish real-time IoT computational tasks. The main observation behind the framework proposed in this paper is that different portions of data streams supporting IoT services may have different relevance to the global computational goal. The framework we propose realizes a cognitive *content-oriented* channel access control, where transmission of concurrent data streams is shaped to create optimal interference patterns to critical IoT data streams. We refer to the former and latter as cognitive and "protected" data streams. However, we remark that in a general formulation the IoT streams can also implement cognitive behaviors.

In most traditional cognitive network frameworks, the notion of cognition was used to identify and use for transmission of empty time/frequency slots, the so called white space [7]. The objective, then, was to make the communications of the different classes of users orthogonal, avoiding interference as much as possible. In modern network coexistence scenarios, the portions of spectrum shared by multiple technologies may be occupied by many users transmitting heavy data streams, such as multimedia information. In this context, the rigid classification of users typical of traditional cognitive network frameworks jointly with a white space-based approach would result in starvation of non-prioritized users.

The framework we propose seeks practical methodologies to control the interference generated by the cognitive wireless nodes to concurrent data streams in a semantic fashion. The transmission pattern of the cognitive users is determined based on the state of the concurrent data streams, defined to describe the relevance of each segment of data being transmitted to the algorithms consuming the data. However, while the binary idle-busy state necessary to control transmission in white space-based approaches can be directly inferred by the cognitive nodes, the semantic information driving transmission decisions in the considered scenario necessitates a sophisticated architecture entailing the collaboration of devices and infrastructure-level agents.

A key component of the proposed architecture is edge computing [8], where computation resources (edge processors) are placed within a one-hop low-latency topology to provide real-time and reliable services within wireless islands. In our proposed architecture, the edge processors support transmission control by analyzing the incoming data streams to extract useful semantic information. The wireless nodes, the cellular resource manager and the edge processor collaborate to build a map of the content state in time/frequency slots occupied by the protected IoT users.

To illustrate the general principle behind the proposed architecture, we consider a case-study scenario where Device-

Part of this work had been published in IEEE GLOBECOM 2016 in [1].

to-Device (D2D) communications coexist with Long-Term Evolution (LTE) cellular communications in the same bandwidth [9]. The chosen application is remote monitoring, where video streams acquired by local sensors are analyzed by the edge processor to detect and classify objects of interest, for instance to identify treats and support autonomous transportation networks. We assume that the IoT data streams transport encoded video over LTE, and that a local, cognitive, D2D link uses for transmission the same channel resource. Interference from the D2D link can severely impair the performance of algorithms processing the video streams in real time. In order to minimize its impact on the decoding and analysis processes performed at the edge processor, the cognitive transmitter exploits the semantic structure of the temporal encoding of the video streams.

The proposed scheme requires the extension of the LTE protocol stack to include the notion of content state, and to implement messaging supporting the content-aware transmission strategy of the cognitive terminals. We conducted our investigations by implementing these modifications within the NS-3 simulation environment. By means of detailed network and data processing simulations, we demonstrate that the proposed content-oriented paradigm can significantly increase the throughput achieved by the D2D transmitter for a given maximum degradation of the processing algorithm output compared to a uniform interference strategy.

The rest of the paper is organized as follows. In Section II, we describe network coexistence in the urban IoT context. Section III describes the considered application and network scenario. Section IV presents the architecture supporting content-aware cognitive interference control. In Section V, we describe and discuss the case study considered in this paper, where D2D communications coexist on the same bandwidth with video streaming over LTE. Section VI presents the experimental simulations and evaluations. In Section VII, we discuss related work in the area of D2D-LTE coexistence. Section VIII concludes the paper.

II. D2D and LTE in the Urban IoT

Due to spectrum scarcity, wireless communication and network technologies are being designed to coexist on the same portion of spectrum. For instance, recent LTE-based cellular networks are proposed to operate in unlicensed 5 GHz band [10] to offload traffic. Since this band, as per IEEE 802.11 standards, is also used by Wi-Fi, an interference control problem arises. The development and increasing popularity of Device-to-Device (D2D) communications further exacerbates the problem of interference, especially in dense urban deployments. Originally, D2D communications were only designed for short range links without infrastructural support. More recently, WiFi direct has been proposed for direct D2D communications between WiFi devices without coordination from a local Access Point (AP).

D2D communications over cellular networks were originally intended as a way to increase network connectivity [11]. Recent studies use this technology to build high data rate, short-range, links between devices and increase spectral efficiency [9,12,13]. Different mechanisms have been proposed

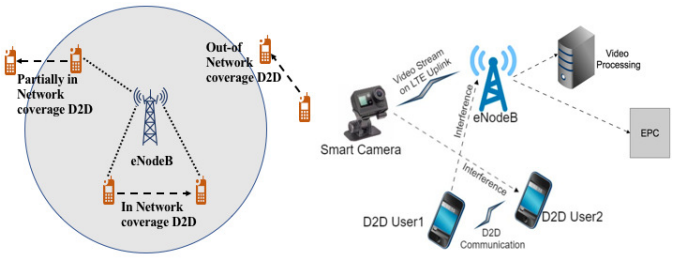

a) D2D in different network coverage scenarios

b) D2D underlay on LTE network with Video Streaming Application on Uplink

Figure 1: D2D scenarios and ProSe architecture in 3GPP LTE.

for this class of D2D communications. Recent work studied D2D communications as an in-band overlay of cellular networks, where a dedicated portion of the spectrum is assigned to D2D communications. However, this family of solutions may not be efficient in terms of bandwidth utilization and is not scalable [14,15]. Alternatively, D2D communications can be deployed in-band, where D2D transmissions underlay the spectrum used by the LTE cellular infrastructure. However, in-band D2D underlay may result in a reduced ability of the network to control interference.

A. D2D in 3GPP LTE

The proliferation of local services (*e.g.*, social networking) led to the inclusion of D2D communications in the recent release 12 of 3GPP [16] as Proximity Services (ProSe). In the LTE standard, the D2D link is defined as a "sidelink" in order to differentiate it from uplink and downlink. The major two features defined in the standard are D2D discovery and D2D data communication. D2D discovery is signaled by the Physical Sidelink Discovery Channel (PSDCH), whose assigned resources are specified by the eNodeB in the Downlink Control Information (DCI). Herein, we do not address the D2D discovery mechanism and, instead, focus on D2D data communication assuming the D2D devices are connected and ready to communicate. Specifically, we consider D2D communications "in-network coverage" or "partially in network coverage" as shown in Fig. 1(a), where the D2D transmitter interferes with uplink LTE transmissions.

Resource allocation can be performed in "scheduled" or "autonomous" mode. In scheduled mode, the eNodeB allocates the resources for D2D links to operate using the Physical Sidelink Control Channel (PSCCH) and Physical Sidelink Shared Channel (PSSCH). In case of in network coverage autonomous resource allocation, the D2D device selects portions of a resource pool preconfigured by eNodeB in the System Information Block (SIB) [16].

III. Problem Statement

In the following, we describe the application scenario and network environment, and state the general objective of the proposed framework.

A. Network and Application Scenario

Although the methodology proposed in this paper can be applied to a wide range of scenarios, we consider a network

setting where data streams are transmitted over Frequency Division Duplex LTE (FDD-LTE) networks for multi-scale processing, and a D2D terminal transfers data using D2D underlay of LTE in the same frequency band as shown in Fig. 1(b). We assume network-assisted D2D communications [17], where the LTE operator assists in establishing the D2D connection through authentication and authorization over E-UTRAN. Once the connection is established, data communication is performed via direct radio rather than through the E-UTRAN infrastructure, which can be used for occasional control and signaling messages. The framework we propose is positioned within the in network coverage autonomous resource allocation configuration, and we assume the cognitive D2D devices use control information from the LTE eNodeB to synchronize with the LTE frame structure.

Data from the LTE User Equipments (UE) are streamed uplink via the Serving Gateway (SGW) and Packet Data Network Gateway (PGW) in the Evolved Packet Core (EPC) network towards a remote host. Herein, we are primarily interested in uplink transmission by E-UTRAN. When the RRC (Radio Resource Control) layer of UE has a Packet Data Unit (PDU) to transmit on uplink, it passes the PDU to the underneath PDCP (Packet Data Convergence Protocol) layer which forwards it to the RLC (Radio Link Control) sublayer. The RLC reports its buffer status to the underlying Medium Access Control (MAC) layer, which transmits a control message to the eNodeB MAC scheduler. The scheduler allocates Resource Blocks (RBs) for data transmission based on the channel quality measured in terms of Signal-to-Interference-plus-Noise-Ratio (SINR) which varies with received signal strength, noise and interference. As per the standard, for LTE uplink, the SINR is measured using a control signal, e.g., the SRS (Sounding Reference Signal), or a data signal, e.g., PUSCH (Physical Uplink Shared Channel), at the eNodeB MAC layer. The eNodeB layer calculates the CQI and reports it to the scheduler. The scheduler selects a suitable MCS and notifies the UE MAC via DCI [18]. The UE MAC then transmits the PDU(s) based on the data rate supported by the assigned MCS. When the D2D link is active in the LTE uplink band, the interference it causes degrades the achievable channel rate of the UEs. If the interference is high, the channel may not be able to support even the lowest MCS, in which case the LTE receiver fails to decode the PDU.

Prior contributions addressing interference control in D2D communications underlaying LTE proposed scheduling and interference control strategies that aim at maintaining the SINR at the LTE receiver above a certain threshold [19]–[21]. However, these techniques require instantaneous channel knowledge for every transmission slot as well as physical layer parameters, and they may not harvest all the available bandwidth in this complex coexistence scenario. Herein, we assume that the D2D transmitter autonomously makes transmission decisions within the assigned spectrum without any prior information on the channel. D2D transmissions interacts with the rate selection mechanism described earlier, and may cause the delayed delivery or loss of PDUs.

B. Problem Formulation

In order to make our description general, we refer to the data transmission slots (subframes in the LTE architecture) as "periods", where the i–th period contains the data generated by the transmitter in the time interval $\tau_i=[t_{i-1}, t_i)$, $i=1, 2, 3, \ldots$, with $t_0=0$. We map each period to a "state", which we denote with S_i. The state describes the content generated by the UEs in the corresponding section to the processing algorithm. We define the finite state space $\mathcal{S}=\{1, \ldots, K\}$, with $S_i \in \mathcal{S}$, $i=1, 2, 3, \ldots$, and the sequence $\mathbf{S}_i^N=(S_{i-N+1}, \ldots, S_i)$. Further, we define the set of packets generated in τ_i as $\mathbf{p}_i$.

Transmission of the D2D transmitter is controlled by a policy μ, which is defined over the same synchronized time periods as the content state of the interfered data streams. The action takes the form of a transmission probability function of the state within each period. The action in the time period i, then, is $a_i=\mu(\mathbf{S}_i, \mathbf{a}_{i-1}) \in \mathcal{A}$, where $\mathcal{A}$ is a finite action set and $\mathbf{a}_i^N=(a_{i-N+1}, \ldots, a_i)$.

The packets generated by the LTE UEs suffer an interference pattern that is a function of the policy. Herein, we assume that the packet loss pattern in τ_i is a (probabilistic) function of the action a_i. For the sake of generality, we say that due to interference, the network transforms the packet sequence $\mathbf{p}_i$ into the sequence $\hat{\mathbf{p}}_i$, where some packets may be missing due to decoding failure, excessive delay, *etc.*

The output of the algorithm depends on the content state and received packet sequences. The performance of the algorithm consuming the incoming data stream is measured by the function $\phi(\hat{\mathbf{p}}, \mathbf{S})$, where $\hat{\mathbf{p}}=(\hat{\mathbf{p}}_1, \hat{\mathbf{p}}_2, \ldots)$. In this paper, we accomplish the following objectives:

Architecture: Develop an architecture supporting content-aware transmission policies capable of: *a)* promptly identifying the content state of incoming data streams; and *b)* notifying D2D transmitters to drive transmission actions.

Transmission Policy: Devise content-aware transmission policies μ controlling the transmission pattern of the D2D users whose objective is to preserve the quality of the output of algorithms processing the data streams, that is, maintain $\phi(\hat{\mathbf{p}}, \mathbf{S})$ above a predefined threshold. In this paper, we use Q-Learning, a popular form of Temporal-Difference learning to identify the optimal transmission, and thus interference, policy. As clarified within the context of the specific scenario considered in this paper, due to the mapping on periods over the time frame of decisions rather than packets as in most prior work in the cognitive networking domain, the action space can include articulated actions corresponding to sub-policies applied within each period.

IV. System Architecture

First, we describe the architecture supporting the content-aware interference policies operated by the D2D link. The system architecture defines the components of the cognitive network and the control and data path for the LTE and D2D messages. Along with those characterizing the LTE stack, the components include a Deep Packet Inspection (DPI) module which interacts with the MAC layer of the LTE UEs, and a cognitive engine which contains a state repository collecting

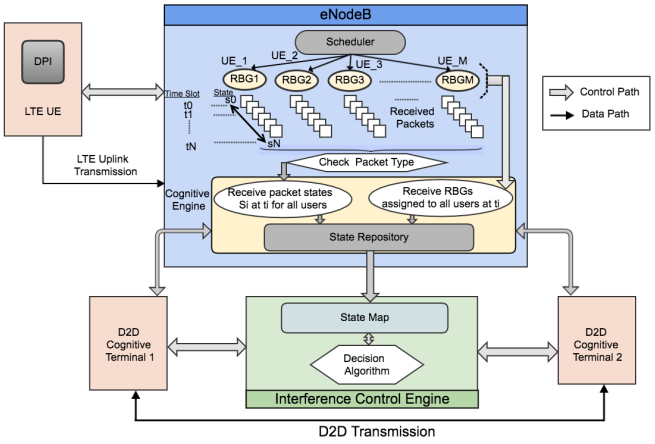

Figure 2: System Architecture for D2D underlay with LTE Uplink Transmission.

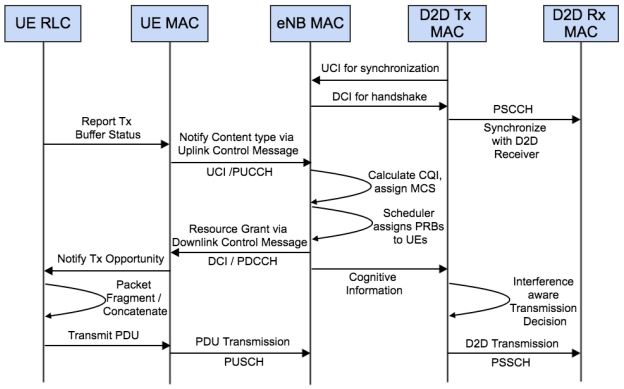

Figure 3: Message flow for LTE Uplink Transmission and coexisting D2D Transmission

the required information for supporting the transmission decision algorithm. In the following, we describe in detail these components, which are summarized in Fig. 2 together with the message flows as described in Fig. 3.

Deep Packet Inspection: The UEs implement a DPI module at the MAC layer to determine the packet type at the source. This functionality allows the early identification of packet classes generated by applications and data encoders. The class might already be a sufficient descriptor of the content state S_i. Later in the paper, we connect this model to a specific scenario, where the type of frame emitted by a video encoder determines the relevance of packets to accomplish a computational objective, which takes the form of object detection and classification. In this case, the "content state" is constituted of the packet type based on the specific encoded data frame it belongs to, and the position of the packet in a frame or group of frames. The UE transmits a control message via the Uplink Control Information (UCI) on Physical Uplink Control Channel (PUCCH) with the content state to the eNodeB which first schedules a Resource Block Group (RBG) to the user and then assigns a MCS based on the CQI as shown in the Fig. 3. The eNodeB sends the content type of the allocated users and the scheduling map to the "cognitive engine" for processing. Note that, the UEs do not report content state for every individual packets, but only when a state change is detected in order to reduce control message overhead for the DPI messages.

Cognitive Engine: The cognitive engine resides in the eNodeB, which collects the content states and resource allocation of the UEs for each transmission period and creates a "State" repository. The eNodeB also collects information regarding the spectrum assigned to the D2D transmitter via UCI and builds an optimized map of the content state in each subframe and LTE channel.

The state repository in the cognitive engine maintains the state of the last N packets for each UE to determine if the next incoming packet belongs to the same continuing period or is the beginning of a new period. Based on the state queue, the cognitive terminals can employ instantaneous or history dependent interference control strategies. The cognitive engine is notified by the D2D terminals regarding the resource pool it is using, and hence, determines the m overlapping UEs out of total M UEs $(m \in M)$ as scheduled in the subframe.

Decision Algorithm: In the context of LTE FDD, one LTE radio frame of 10 ms duration is divided into 10 subframes of 1 ms duration each and each subframe contains 2 slots of 0.5 ms. The radio resources are allocated in terms of Physical resource block (PRB) [18] of 12 subcarriers such that each slot of 0.5 ms contains a number of PRBs. The decision algorithm controls the transmission of the D2D link in each subframe based on the interference control strategy. Thus, the action set $\mathcal{A}$ corresponds to transmission probabilities ρ_i within individual subframes. For simplicity, we assume that D2D transmissions occupy the whole assigned spectrum of the resource pool. However, the transmission policy can be extended to include the dynamic selection of one or a subset of channels based on the state map.

Fig. 4 shows an example of packet flow of one protected and multiple cognitive data streams in the cognitive system architecture. The proposed content-oriented policies shape the transmission process of the cognitive nodes to create interference patterns compatible with the interfered data stream and its processing.

We define two classes of heuristic transmission strategies: Past Independent and Past Dependent protocols.

Past Independent Protocols: In this first class of policies, we define control actions solely on the content state in each individual period S_i.

Past Dependent Protocols: In this second class of policies, the decision in period i are a function of the state sequence $\mathbf{S}_i^N = (S_{i-N+1}, \ldots, S_i)$.

These policies are compared with those obtained by means of Dynamic Programming techniques maximizing a global reward function evaluated at the edge processor.

V. Case-Study Scenario

In order to illustrate its performance, we present an implementation of the proposed framework in a specific scenario, where the video stream from a surveillance camera

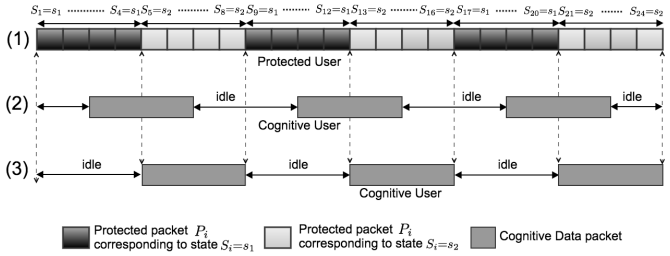

Figure 4: Cognitive controlled transmission (1) Protected packet flow, (2) Content-agnostic cognitive packet flow, (3) Content-aware cognitive packet flow

is processed by the edge processor to identify objects within the individual frames. Referring to the network infrastructure described earlier, the, protected, video streams are transported over LTE, which is interfered by a cognitive D2D link. We contend that LTE network for the video transmission is an appropriate choice, as LTE has high bandwidth and range of communication, and also has dedicated uplink channel for upstreaming the data to the edge processor.

A. Video Streaming:

A video is a sequence of images produced at a given rate. Unlike images, which only have a spatial component, a video has a temporal component as well. Therefore, compression is performed both along the spatial and temporal dimensions.

Spatial compression: The individual pictures are partitioned into "macroblocks" which are transformed by Discrete Cosine Transform (DCT) from space domain to frequency domain. Basic MPEG-4 uses 8×8 DCT whereas H.264/MPEG-4 Advanced Video Coding (AVC) standard uses a 4×4 DCT-like integer transform. The transformed data, then, are quantized and encoded using entropy coding.

Temporal compression: Temporal compression exploits the significant similarities that may interest pictures within the video stream captured at close time instant. This gives the opportunity to encode the video in a smaller number of key (reference) frames and a larger number of differential frames following the reference frame, which encode differences with respect to neighboring reference frames. Thus, in order to decode differential frames, the decoder also uses the associated reference frame(s).

When an encoded frame is damaged, that is, packets transporting fragments of it are lost or received with excessive delay, due to spatial compression, the decoding process results in the multifold corruption of the output image content and resolution. The spatial propagation of errors may create artifacts that are detected as objects, or impair the ability of the algorithm to detect existing objects. Additionally, due to temporal compression, if a reference frame is damaged, the effect propagates through the entire Group of Pictures (GoP) defined as a reference frame and a set of dependent differential frames. Conversely, if a differential frame is damaged, the effect remains localized to the frame[1], as some information regarding motion vectors may be lost, but key features in following frames are decodable. Herein, we consider H.264/AVC

[1]Although some dependencies may exist across differential frames

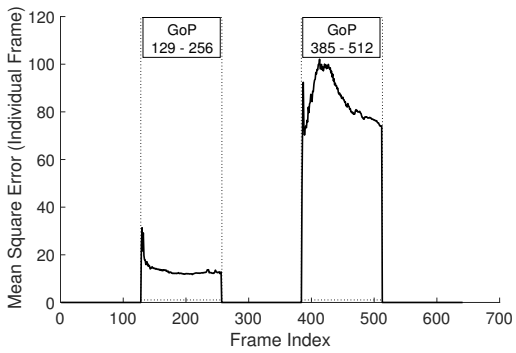

Figure 5: MSE as a function of the frame index. The I-frames with indexes 129 and 385 are heavily damaged and the error propagates through the entire GOP (128 frames).

encoding, where GoP starts with intra-coded frame (I-frame) followed by a number of inter coded differential frames (D-frame), that is, Predicted frames (P-frames), Bi-directional predicted frames (B-frames) and can be of constant size or variable size.

To illustrate error propagation in a GoP, we emulated the effect on a real-world video from a surveillance camera. The video is composed of 641 frames and is highly compressible, with fixed GOP size equal to 128 frames. Each frame is composed of 640x360 pixels. In Fig. 5, we show the impact of the loss of the I-frames with indexes 129 and 385 on the per frame Mean Squared Error (MSE) of the video. The error propagation effect is perceivable. Thus, D2D transmission during a reference frame transmission carries a larger amount of "effective interference" to the computing algorithm compared to the same transmission during differential frames. Note that artifacts caused by damage to reference frames may persist during the entire GoP and mislead object tracking algorithms to categorize them as objects.

Based on this observation, we define content classes which include a flag discriminating between reference and differential frames. Thus, we build the notion of relevance of packets within periods of the data stream based on the semantic structure of the data stream itself. In a more general definition, the content class within periods could be defined by the presence of objects of interest (*e.g.*, pedestrians), and the state would need to be extracted by the edge processor.

In the considered case, the LTE UEs transmitting the video stream sends a preamble message with the control information on the uplink to the eNodeB reporting the frame type (I, B/P). As a GoP contains a series of frames and each frame contains hundreds of packets, it is sufficient to send the frame type at the first packet of each frame instead of in all the packets in that frame. An increased robustness with respect to packet loss can be achieved by repeating the frame type information in more than one packet at the beginning of each frame.

B. Performance Metrics

We evaluate the performance of the proposed scheme by measuring the accuracy obtained by object detection and recognition algorithms applied to the resulting video stream.

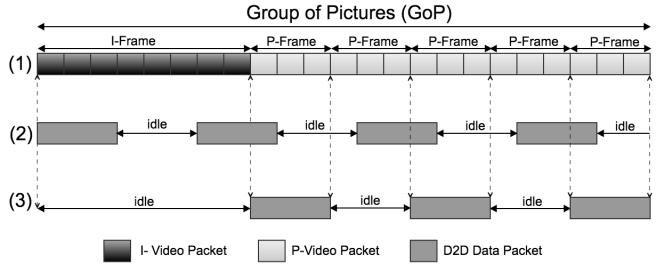

Figure 6: Cognitive Interference Strategies: 1) Video packet flow; 2) Fixed D2D Tx probability; and 3) FDTP.

1) Object Detection: Object detection is one of the primary applications in computer vision. Most object detection algorithms extract features from the image frames and employ a matching or detection algorithm with respect to reference images. In this paper, for the purpose of illustration and performance evaluation, we use the Speeded Up Robust Features (SURF) based object detection technique [22] to detect the surface point of objects in each frame of a video with respect to a reference image. So, as interference corrupts the video and affects object detection, we measure the object detection rate as:

$$P_{det} = \frac{N_{rcv}}{N_{ref}} \tag{1}$$

where N_{rcv} and N_{ref} are number of correctly detected surface objects in the received and reference video respectively such that $\{N_{rcv}, N_{ref}\} \in N_{orig}$ where N_{orig} is the feature set detected in the original uncorrupted video.

2) Object Recognition Quality: We also measure the object recognition quality where specific objects are recognized using a classifier trained with a gaussian mixture model [23]. We emphasize that any algorithm in this class is likely to be heavily affected by corruption of the video. In fact, blurred portions of the image, especially when correlated errors occur in the image sequence, can lead the algorithm to detect non-existing objects. Although it is difficult to define a general metric for object recognition, we can measure the object recognition rate, positive prediction rate and the false positive rate with respect to the uncorrupted video based on the "true positive (T^p)", "false negative (F^n)" and "false positive (F^p)" detection as described in [24]:

$$\begin{aligned} Object\ Recognition\ Rate &= \frac{T^p}{T_0^p}\ , \\ Positive\ Prediction\ Rate &= \frac{T^p}{T^p + F^n}\ , \\ False\ Positive\ Rate &= \frac{F^p}{TF}\ , \end{aligned} \tag{2}$$

where $\mathrm{T}_0^{\mathrm{p}}$ is detected objects in base video and TF is the Total number of Frames.

To measure T^p, F^p and F^n, we compare the object recognition of the corrupted video with the reference video frame by frame. Let N_o be the number of objects recognized in the original video in the frame F. In the corrupted video, the total number of objects recognized is M_o. Then, based on how many objects in N_o correspond to the objects in M_o within an error margin equal to δ, we count $m_o \epsilon M_o$ corresponding objects as true positive for that frame F. The $(M_o - m_o)$ objects which are recognized in the corrupted video but not in the original video are counted as false positive. One point to be noted here that the true negative is 0 as we don't track objects that are not detected. However, false negatives can be found by the objects which are detected in the original video but not present in the corrupted video. So, $(N_o - m_o)$ gives number of false negatives.

3) Efficiency: : We define the efficiency of the control policy as the ratio

$$\text{Efficiency} = \frac{D_{avg}}{1 - T_{d2d}}. \tag{3}$$

where D_{avg} is average object detection rate and T_{d2d} is the throughput of the D2D link. Higher efficiency indicates that the LTE UEs achieve high object detection rate, but also provide transmission opportunities to the cognitive D2D terminal.

C. Interference Control Strategies

First, we seek the optimal transmission strategy of the D2D link by means of Q-Learning [25], a widely used Temporal Difference Learning Framework. In the considered scenario, we consider a case with one active UE and define states and actions at the temporal scale of GoPs, that is, a reference frame followed by a sequence of differentially encoded frames. Due to the independence between GoPs, the state space is composed of one state only. The simplicity of the state space contrasts with the complexity of actions, which define articulate transmission patterns over the GoP and the associated section of packet stream. In particular, each action is associated with the parameters of two binary Markov chains controlling the transmission pattern of the D2D link in the sections of GoP transporting reference and differential frames. The states of the Markov chain correspond to an idle (state 0) and active (state 1) D2D link, and the global action determines the transmission probability $e = \frac{p_{01}}{p_{10}+p_{01}}$ and average transmission burst size $B = 1/p_{10}$, where p_{ij} is the transition probability between state i and $j \in \{0, 1\}$. A finite set of actions is obtained by defining a set of e and B parameters for the two chains. A standard Q-Learning algorithm is used to identify the action with the maximum Q-Value computed based on the reward function

$$R(a) = \lambda R_{D2D}(a) + (1 - \lambda) R_{LTE}(a) \tag{4}$$

where a is the action in the action space $\mathcal{A}$, $R_{D2D}(a)$ and $R_{LTE}(a)$ are the rewards corresponding to the utility of the D2D and LTE links, respectively, and $\lambda \in [0, 1]$ is a weight parameter. In the considered case. we define $R_{D2D}(a)$ and $R_{LTE}(a)$ as the normalized throughput of the D2D link within the GoP and the average PSNR of the transmitted frames, respectively.

We now instantiate the past independent and dependent policies for the case-study scenario and LTE network environment we described earlier. The policy determines transmission probability within the LTE frames contained in the time period

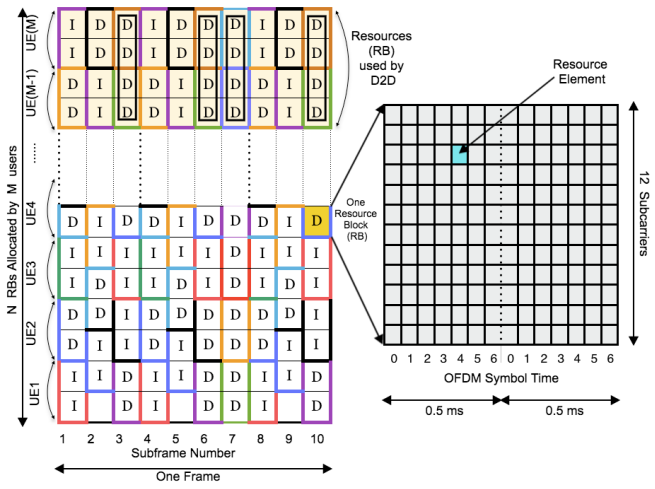

Figure 7: State map in a LTE frame with multiple UEs transmitting video frames.

associated with a data class. Fig. 6 provides a graphical representation of the policies presented in this paper.

In practical scenarios, several UEs transmitting data stream over LTE can share the spectrum with the D2D link. Let us denote the total number of LTE users in the cell as M and total number of resource blocks (RB) in the spectrum as N. So, on average each user is assigned $k = \lfloor N/M \rfloor$ RBs. Suppose, the D2D transmitter uses a resource pool of l RBs (which are usually consecutive). If $(l < k)$, then resources for only one UE (k RBs) will overlap the entire resource pool and the transmission decision of the D2D terminal will be solely based on that specific user's content state. However, when $(l > k)$, then, the D2D link's transmission decision will be based on more than one overlapping UEs' content type. To be specific, the transmission probability will be dependent on content state of m users where $m = \lceil l/k \rceil$ and $(m \in M)$. The values of k and l are variable; k decreases as number of users M increases and resource pool size l is selected by the D2D. Fig. 7 illustrates the resource usage scheme.

The state map, then, is defined to capture the frame type in each subframe and channel, that is, the state in subframe i and RB n is $S_{i,n} \in \{I, D\}$, where I and D correspond to a subframe and RB in which a reference and a differential frame are transmitted, respectively. The state S_i, then, is the vector $S_i = [S_{i,1}, \ldots, S_{i,N}]$.

Frame Dependent Transmission Probability (FDTP): In this past independent protocol, the D2D transmitter selects the transmission probability depending on whether the LTE UEs, are transmitting reference (I) or differential (D) frames in the current subframe. Herein, we simplify the decision policy, and define the transmission probabilities ρ_I and ρ_D, corresponding to subframes where at least one RB is assigned to a UE transmitting an I frame and to subframes where all RB are assigned to UEs transmitting D frames, respectively.

We observe that in a scenario where the spectrum assigned to the D2D link overlaps with multiple UEs, there might be the risk of starvation. In fact, the I frames of the various UEs can create a thread in which only few subframes exist where all the RBs are assigned to differential frames. To mitigate this issue, more involved policies could be defined to map increasing transmission probability to a decreasing number of RB assigned to UE transmitting I frames.

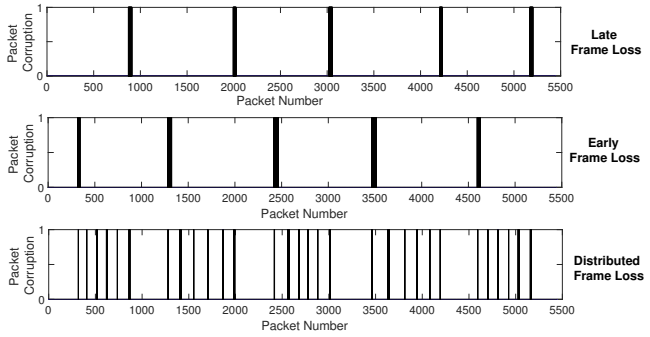

Figure 8: History-based interference strategies with different spacing.

Frame History Transmission Probability (FHTP): In the FHTP policy, the system exploits the information contained in the state repository, that is, a sequence of past states. With respect to FDTP, we extend the definition of state to include the distance of the corresponding frame within the GoP. The objective is to finely tune the transmission pattern and minimize the impact of interference on the processing algorithms.

First, we analyze the impact of packet loss induced by interference within a frame. Similar to FDTP, we keep subframes transporting reference frames free of interference, and we restrict transmission from the D2D link in subframes associated with PDUs part of differential frames. Unlike FDTP, we concentrate interference bursts in specific differential frames, thus having a smaller number of frames affected by packet loss within each GoP. We experimentally measure the effect of specific patterns with different distribution of frames affected by interference bursts within the test video. We select affected frames according to three different patterns; "*Late frame loss*", where we select frames towards the end of GoP to damage, "*Early frame loss*", where we select affected differential frames from the earlier part of the GoP, and "*Distributed frame loss*", where we select affected differential frames at regular intervals within GoP.

Fig. 8 shows the packet loss patterns for a number of affected frames equal to 6 in each GoP. We measure the Peak Signal to Noise Ratio (PSNR) to compare the resulting video quality. As each frame contains a variable number of packets, we plot the PSNR against packet loss percentage, where we consider a number of affected frames equal to $6, 10, 15$ and 20. Fig. 9 shows that the late frame loss distribution achieves better PSNR compared to early frame loss and distributed frame loss. However, since packet loss in the video corresponds to D2D link transmissions, the distribution also determines its QoS measures. It can be noticed that both the early and late frame loss induce longer idle periods of the cognitive D2D transmitter, which result in larger packet delivery delay. Conversely, distributed frame loss creates transmission opportunities for the D2D link at shorter and regular intervals when differential frames are being transmitted. Hence, we select

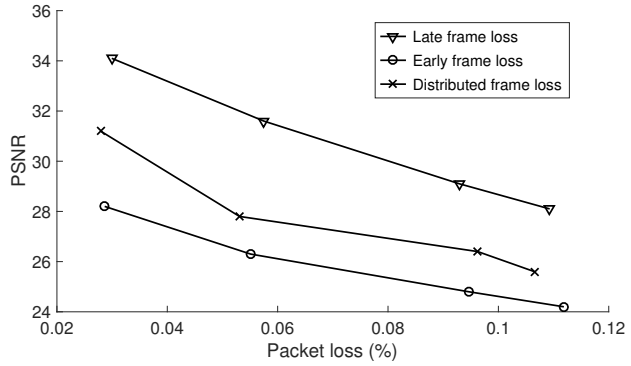

Figure 9: PSNR as a function of packet loss for different transmission patterns.

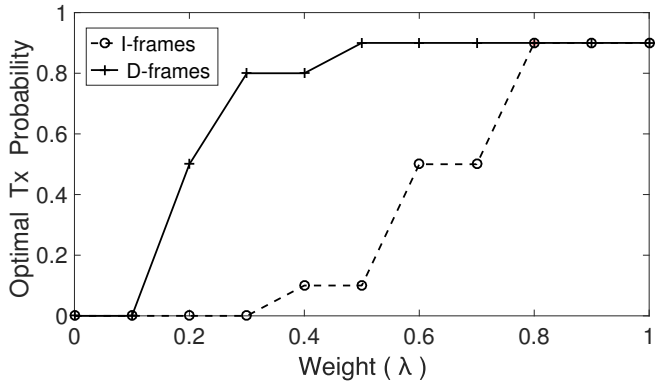

Figure 10: Optimal transmission probability as function of the weight λ. The transmission burst size is taken as fixed = 2.

the distributed frame loss interference, which provides a good tradeoff between video reconstruction quality and performance of the D2D link.

In order to create this class of interference patterns, we add to the state stored in the repository a descriptor of the damage incurred by specific frames within the GoP. For the sake of exposition, we consider a case in which all the RBs used by the D2D link are assigned to one UEs. Thus, the vector S_i can be collapsed to a single variable. To create the desired pattern, we define, then, $S_i{=}(F_i, D_i)$, where $F_i{\in}\{I, D\}$ is the frame type, and D_i indicates the distance of the corresponding frame in the current GoP. The cognitive engine processes the state sequence contained in the repository to create the wanted pattern. The complexity and computation overhead of the FHTP algorithm is higher compared to FDTP as the cognitive engine in FHTP needs to store a number of states equal to the GoP length the state repository.

VI. Numerical Results

First, we show the optimal policy for a case with one UE. For simplicity, we fix the burstiness parameter and only control the transmission probability in the reference and differential frames. Fig. 10 shows the optimal transmission probability as a function of the weight λ. As expected, the learning framework selects idleness when λ is equal to 0 and then progressively increases the transmission probability in the differential frames as λ increases. At saturation, the optimal policy then activates transmission in reference frames. Note that the same structure

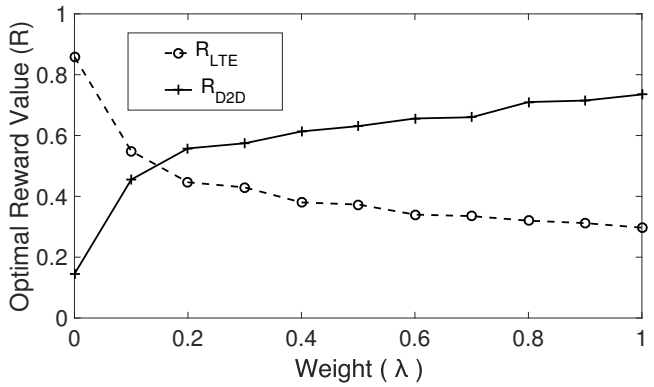

Figure 11: Optimal accumulated reward as function of the weight λ.

of the policy was shown in [26]. Fig. 11 shows how the accumulated reward value of the primary and secondary users follow opposite trends with respect to the variation of weight λ based on the reward function mentioned in equation [4].

We compare the policies proposed herein against a simple scheme where the D2D node predetermines transmission power and access probability ρ to induce a fixed average failure probability to LTE packets. Then, in each slot the D2D terminal transmits with probability ρ with a predetermined transmission power. We refer to this strategy as Fixed Probability (FP). Note that such policies could also be the results of imperfect SINR control, where packet loss is spread across the stream.

We assess the performance of the proposed schemes in the case-study scenario described in Section V by means of detailed network simulation. We use NS-3 version 3.23 [27] with LTE protocol stack to simulate the considered D2D and LTE scenario. In our simulations, D2D shares a portion (set of sub-channels) of LTE uplink spectrum. First, we packetize the video with ffmpeg to generate the transport streams, which are input to the NS-3 simulator with a full end-to-end topology over the LTE protocol stack. The packet loss pattern is applied to the received video, which is, then, decoded and fed to the object detection algorithm implemented in MATLAB. The parameters used in the experiments are reported in Table I.

As we consider real-time delay sensitive application, we disable Hybrid Automatic Retransmission Request (HARQ) and use RLC Unacknowledge Mode (UM). We will explore the effect of HARQ strategies on the proposed framework and

LTE Parameters	**Value**
MAC Scheduler	Proportional Fair (PF)
RLC mode	RLC UM
eNodeB power	25 dBm
UE Tx power	15 dBm
D2D Tx Power	7.5 dBm
Antenna Model	SISO
Path Loss model	Friis Propagation Loss
Uplink EARFCN	18100
UE-eNodeB distance	200 m
eNodeB - D2D distance	1500m
D2D nodes distance	20 m

Table I: LTE parameters for NS-3 simulation.

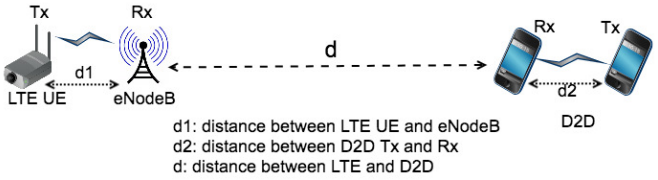

Figure 12: Topology of the LTE and D2D links considered in the results.

video processing scenario in future work. The interested reader can find in [28] a discussion and evaluation of HARQ and video streaming. We use the channel fading trace Extended Pedestrian A model (EPA) on NS-3 as indicated in the 3GPP standard. To simulate the application layer, we build a transport stream of the video composed of a sequence of packets of equal size 188 bytes, which we transmit via UDP. First, we conduct experiments with one LTE UE sharing the spectrum with the D2D transmission. In this setup, we show the performance variation with respect to the network topology, transmission power and mobility. Then, we measure the performance in a scenario with multiple active UEs, where the D2D link is assigned a subset of LTE frequencies.

Topology: Fig. 12 illustrates the line topology used in simulations. The distance between the UE and eNodeB and the D2D transmitter and its receiver are $d1$ and $d2$, respectively. We keep $d1$ and $d2$ fixed and vary the distance d between the eNodeB and the D2D receiver. First, we create a low-interference regime between the D2D and the LTE links by setting the topology parameters to obtain an average LTE video packet loss of 4% when the D2D link is active. Then, we reduce the distance d to create a high interference regime with average LTE video packet loss of 9% when the D2D link is active. For these two regimes, we obtain curves corresponding to different transmission probabilities of the D2D user. Fig. 13 plots the resulting object detection rate as a function of the D2D link's throughput. It can be observed that, in the high interference regime, the baseline protocol (FP) achieves object detection rate below 0.5 even with D2D throughput less than 10%, and then sharply decreases as the D2D link throughput increases. The low interference regime results in a less steep decrease, but still the object detection probability is heavily impacted as the D2D link becomes more active. The FDTP algorithm achieves a much smaller deterioration of the object detection rate, which saturates at approximately 0.4 with a 30% gain with respect to FP in high interference regime. For a given throughput, the past dependent FHTP achieves a performance gain of 35% over FP, and a perceivable gain compared to FDTP. In the low interference regime, FDTP and FHTP outperform FP by approximately 60% and 70% on average, respectively.

Transmission Power: We perform an analogous experiment, where we define the low and high-interference regimes by varying the transmission power of the D2D link instead of the topology. The two interference regimes have the same packet loss probability at the LTE receiver given that the transmitter is active or idle. It can be observed that for any fixed throughput all the protocols improve the achieved object

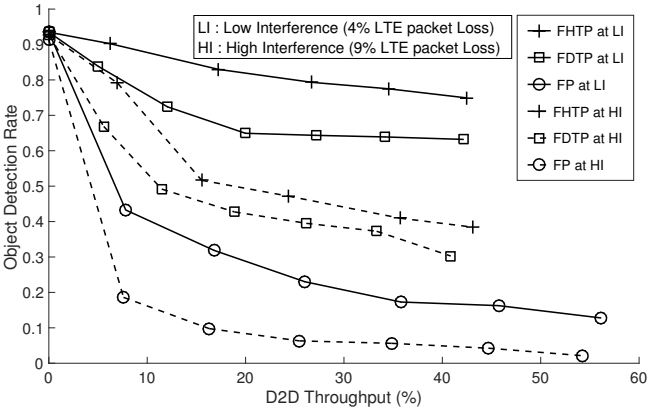

Figure 13: Object detection rate as a function of the throughput of the D2D link. The points in the curves are obtained by changing the transmission rate of the D2D transmitter.

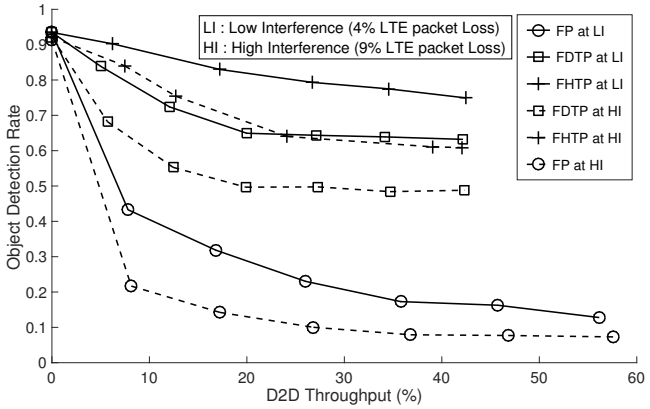

Figure 14: Object detection as a function of the throughput of the D2D link. The points in the curves are obtained by changing the transmission rate of the D2D transmitter.

detection compared to that obtained by changing the topology. However, both FDTP and FHTP further increase the gap with respect to FP, which amounts to 45% and 60%, respectively.

Intuitively, for a set of fixed parameters, a reduced distance between the D2D and LTE links increases the interference at the D2D receiver, thus reducing the achieved throughput of the D2D link, whereas, increasing D2D power to achieve high interference regime will enhance the D2D throughput. Hence, for a given D2D throughput the LTE throughput will be boosted in the latter case.

Mobility: We measure the performance of the object detection algorithm in a setting where users change their positions over time. In particular, the D2D node moves according to a random walk mobility model in a $50\text{m}\times50\text{m}$ grid with uniform speed of 20m/s and 50m/s respectively. Fig. 15 shows that all the protocols are affected by mobility, with a increasing degradation of the object detection rate as the speed is increased. However, even with high mobility, the FDTP and FHTP transmission schemes achieve a gain of 40% and 50% over FP, respectively.

Object Recognition Accuracy: As mentioned earlier, we include in our numerical evaluation object recognition based on Gaussian mixture model from the MATLAB Computer Vision

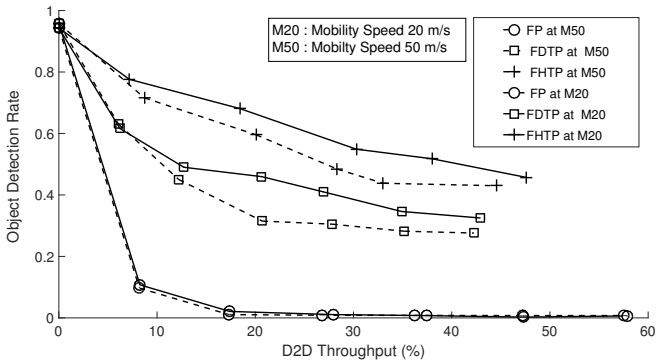

Figure 15: Object detection as a function of D2D throughput in presence of mobility. The points in the curves are obtained by changing the transmission rate of the D2D transmitter.

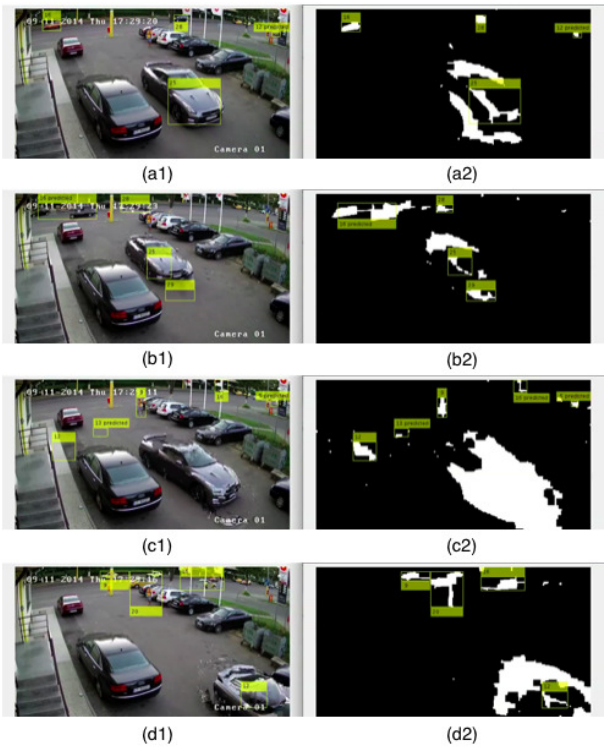

Figure 16: Selected frames from Object recognition of video where objects are detected based on background separation and classified based on a pre-trained model.

System Toolbox. The accuracy of the classifier depends on the number of mixture components, foreground noise during segmentation and also the size range of the bounding box defining the objects.

Fig. 16 depicts the output of the algorithm for the recognition of moving objects, which, based on training from previous video frames, excludes static background objects by segmentation. In Fig. 16.a1, b1, c1 and d1 show frames from the video and a2, b2, c2, d2 are corresponding foreground masks obtained by background separation. Fig. 16.a1 and a2 show the correct object detection. In Figure. 16.b1 and b2, it can be noticed that the shadow of the moving car is detected as a separate object which indicates a false positive. In Fig. 16 c1 and c2, the algorithm detects two objects where objects are

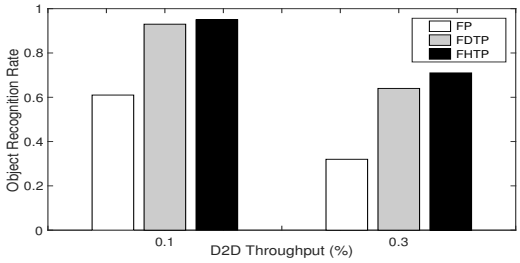

(a) Object Recognition Rate

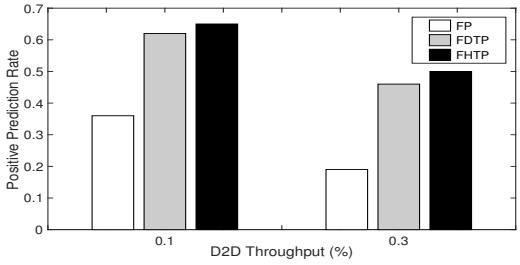

(b) Positive Prediction Rate

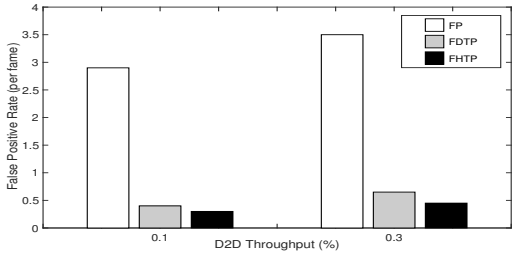

(c) False positive rate

Figure 17: Comparison of object recognition rate, positive prediction rate and false positive rate achieved for FP, FDTP and FHTP.

not present and one false negative as it does not detect the moving car in the middle. In Fig. 16.d1 and d2, the algorithm recognizes all the moving objects. However, due to corruption in the image (near the tail of the moving car at the bottom of the image), the centroid is shifted.

We measure the accuracy of object recognition from lossy video in an interference regime where D2D transmission causes 4% packet loss at the LTE receiver. We chose a topology corresponding to 10% and 30% D2D link throughput and measure the object recognition metrics achieved by FP, FDTP and FHTP.

Fig. 17(a) depicts the object recognition for the FP, FDTP and FHTP protocols. The large gain granted by FDTP and FHTP with respect to FP is apparent in both the settings. Fig. 17(b) shows that the positive prediction rate is also significantly improved by FDTP and FHTP compared to FP. In both cases, the absolute value of the recognition rate and the positive prediction reduces with the increase of D2D link throughput due to the larger packet loss affecting the video stream. Fig. 17(c) depicts the false positive rate per frame. Again FDTP and FHTP outperform FP, as the corruption of frames due to the larger effective interference associated with packet loss in reference frames induces the detection of non-existing objects in the foreground. In all cases, the introduction

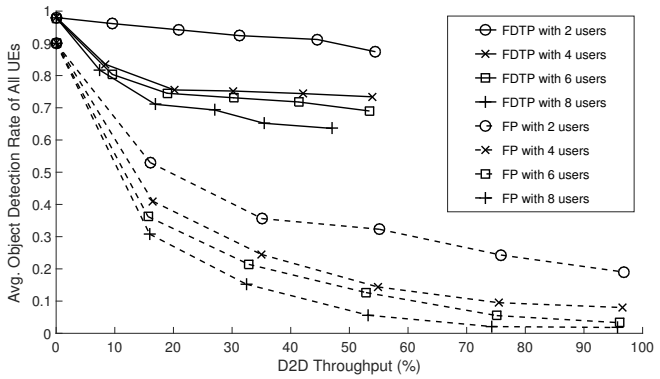

Figure 18: Object detection as a function of D2D throughput with varying number of LTE UEs when D2D uses fixed 6 PRBs. The points in the curves are obtained by changing the transmission rate of the D2D transmitter.

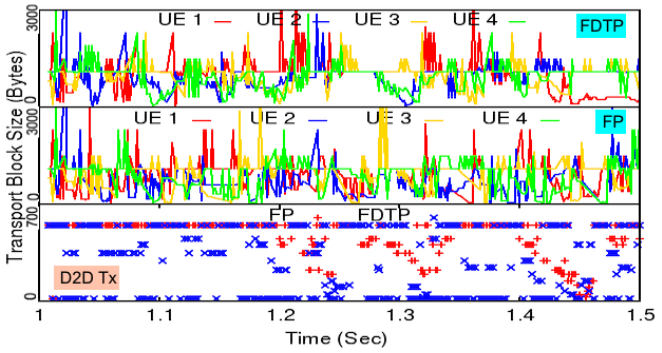

Figure 19: Transport Block allocation map for 4 UEs and D2D link in FP and FDTP. The plot is obtained when D2D always transmits when all of the UE has differential frames.

of memory in the system cognition of FHTP improves the performance of the algorithm.

Efficiency: The efficiency measure defined in Sec. V-B is a function of the D2D link transmission probability and power. Intuitively, increasing the transmission power or the transmission probability of the D2D link increases its achieved throughput. However, it also results in a larger degradation of the object detection rate of the video over LTE. In results not shown here due to space constraints, we found that in order to achieve high efficiency, the FP protocol needs to drastically reduce the transmission probability of the D2D link for any value of the transmission power. Consequently, high efficiency is obtained in a region where the throughput achieved by the D2D link is small. Conversely, FDTP and FDHP maximize the efficiency when transmitting with high probability, but relatively small power (6-8 dBm). Thus, the maximum efficiency is achieved in regions where the D2D link occupies large portions of the channel while collecting throughput even when transmitting with low power thanks to its compact topology.

Multi-UE scenario: First we assign a fixed resource pool (6 PRBs) to the D2D link and vary the number of LTE UEs. We positioned the UEs in a uniform circle and adjusted the initial

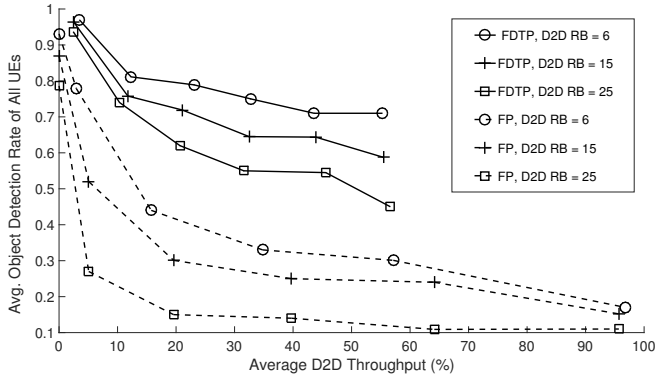

Figure 20: Object detection as a function of D2D throughput with 4 LTE UEs and varying D2D resource pool sizes. The points in the curves are obtained by changing the transmission rate of the D2D transmitter.

transmission power of the UEs to have a maximum packet loss equal to 3.5% when the D2D link continuously transmits. Fig. 18 shows the resulting average object detection rate across the UEs. It can be seen that as the number of UEs increases, the average object detection probability decreases. However, the FDTP gain with respect to FP is about 40%. Noticeably, the absolute value of the D2D throughput decreases as the number of UEs increases due to the larger probability of having at least one sub-channel allocated to an I frame. To illustrate this effect, in Fig. 19 we depict the allocated transport block (TB) size for 4 UEs and the D2D terminal when the D2D transmits with $\rho = 1$. The bottom plot indicates that the D2D transmitters backs off more if FDTP is used compared to FP, as the former does not transmit if any UE is transmitting an I-frame transmitted.

We also studied the effect of the size of the resource pool assigned to the D2D transmitter. For a setting with 4 LTE UEs, we tested a resource pool size equal to 6, 15 and 25 RBs, respectively, and measured the average object detection rate achieved by FDTP and FP as shown in the Fig. 20. FDTP achieves about 40% gain over FP, and the average object detection rate decreases as the resource pool size increases.

VII. Related Work

A significant body of recent research exists which addresses D2D communications over cellular [29] and LTE networks [30]. The notion of cognition has also been studied to alleviate spectrum sharing issues in D2D communications using various resource allocation techniques [1,26,31,32].

Interference control in D2D underlaying LTE: Several techniques have been proposed to mitigate mutual interference between LTE uplink and D2D communications including differentiated scheduling and QoS-aware scheduling. In [33], Doppler *et al.* proposed a mode selection mechanism where the D2D transmitter selects a mode of communication in a set, *e.g.*, using shared spectrum or dedicated spectrum or communicating using the cellular infrastructure. It is shown that learning the strategy even in a single cell environment can improve mode selection in multi-cell environments. Another study investigated mode selection via a relay node [34], where

the D2D link performs transmission either using uplink overlay or underlay to control interference. A distributed power control mechanism was proposed in [35] which uses path loss measurements to control the transmission power of D2D devices. All these studies aimed at optimizing the network performance based on the overall network utilization, but did not specifically consider the performance of real-time services.

Coexistence of wireless technologies: Recent paradigms, *e.g.*, LTE-Unlicensed (LTE-U), Licensed Assisted Access (LAA) [36], propose LTE transmissions in unlicensed bands. The coexistence of LTE with other technologies with non-centralized architectures, such as WiFi, in unlicensed bands, poses several challenges, whose solution requires sophisticated techniques to control mutual interference. Qualcomm proposed a technique called Carrier Sensed Adaptive Transmission (CSAT) [37], where LTE operates with an adaptive duty cycle. The LAA standard uses an energy detection-based Listen-Before-Talk (LBT) mechanism [38], which is coupled with Clear Channel Access (CCA). Another technique called Almost Blank Subframe (ABS) was proposed in [39], which reduces the power and activity in selected downlink subframes to favor coexisting WiFi transmission in the same spectrum. The goal of all these protocols is to improve overall network throughput by maintaining the fairness of LTE and WiFi access.

Adaptive Video Transmission: Adaptive video transmission mechanisms, *e.g.*, HTTP Live Streaming (HLS) [40] and Dynamic Adaptive Streaming over HTTP (DASH) [41] were developed in recent years to provide reliable video transmission against variations in the capacity of wireless links. However, these protocols are based on TCP, which may incur an excessive delay in real-time applications. Moreover, these techniques are most suited to the streaming of stored video, due to the need to create multiple versions of it with different quality. Moreover, current video processing algorithms assume a fixed quality and resolution of the input. Finally, adaptive GoP can dynamically vary the compression rate. However, it would likely create highly compressed segments missing features important to achieve high quality of the output of the processing algorithm.

Edge-assisted Computation for real-time applications: The interested reader can find an in-depth discussion of the challenges of real-time applications, *e.g.*, video streaming, over wireless networks in [42]. To address these issues in complex urban IoT and Smart City environments, applications such as smart transportation (*e.g.*, traffic monitoring) and surveillance systems [43] adopt edge-computing solutions. In this context, edge-assisted architectures for video surveillance over wireless networks were proposed in [44].

VIII. Conclusions

In this paper, we proposed a content-based cognitive transmission strategy for hybrid D2D/LTE networks supporting urban IoT applications. A monitoring application was considered, where video data streams are remotely processed to detect relevant objects. The proposed cognitive strategy shapes the transmission strategy to match the structure of video encoding and processing. Numerical results show significant throughput gain of the D2D link for a given performance degradation of the monitoring application with respect to the case when the interference process is fixed throughout the video transmission. In future work, we will consider more articulated scenarios, such as object detection from a multiple smart cameras, more sophisticated computer vision algorithms and intelligent HARQ mechanisms which can further improve real-time applications for public safety and monitoring.

References

[1] S. Baidya and M. Levorato, "Content-based Cognitive Interference Control for City Monitoring Applications in the Urban IoT," *IEEE Global Communications Conference, (GLOBECOM) 2016, Washington DC, USA, December 4-8*, 2016.

[2] L. Atzori, A. Iera, and G. Morabito, "The internet of things: A survey," *Computer networks*, vol. 54, no. 15, pp. 2787–2805, 2010.

[3] A. Zanella, N. Bui, A. Castellani, L. Vangelista, and M. Zorzi, "Internet of things for smart cities," *IEEE Internet of Things Journal*, vol. 1, no. 1, pp. 22–32, 2014.

[4] P. Bellavista, G. Cardone, A. Corradi, and L. Foschini, "Convergence of MANET and WSN in IoT urban scenarios," *IEEE Sensors Journal*, vol. 13, no. 10, pp. 3558–3567, 2013.

[5] J. Mitola, "Cognitive radio: an integrated agent architecture for software-defined radio," Doctor of Technology, Royal Inst. Technol. (KTH), Stockholm, Sweden, 2000.

[6] B. Manoj, R. R. Rao, and M. Zorzi, "Cognet: a cognitive complete knowledge network system," *IEEE Wireless Communications*, vol. 15, no. 6, pp. 81–88, 2008.

[7] S. Geirhofer, L. Tong, and B. M. Sadler, "Cognitive radios for dynamic spectrum access-dynamic spectrum access in the time domain: Modeling and exploiting white space," *IEEE Communications Magazine*, vol. 45, no. 5, 2007.

[8] F. Bonomi, R. Milito, J. Zhu, and S. Addepalli, "Fog computing and its role in the internet of things," in *Proceedings of the First Edition of the MCC Workshop on Mobile Cloud Computing*, ser. MCC '12, 2012, pp. 13–16.

[9] K. Doppler, M. Rinne, C. Wijting, C. B. Ribeiro, and K. Hugl, "Device-to-device communication as an underlay to lte-advanced networks," *IEEE Communications Magazine*, vol. 47, no. 12, pp. 42–49, Dec 2009.

[10] R. Zhang, M. Wang, L. X. Cai, Z. Zheng, X. Shen, and L.-L. Xie, "Lte-unlicensed: the future of spectrum aggregation for cellular networks," *IEEE Wireless Communications*, vol. 22, no. 3, pp. 150–159, 2015.

[11] Y. Lin and Y. Hsu, "Multihop cellular: A new architecture for wireless communications," *in Proc. IEEE INFOCOM, 2000, vol. 3, pp. 1273-1282*, 2000.

[12] B.Kaufman and B.Aazhang, "Cellular networks with an overlaid device to device network," *in Proc. Asilomar Conf. Signals, Syst. Comput., 2008, pp. 1537-1541*, 2008.

[13] T. Peng, Q. Lu, H. Wang, S. Xu, and W. Wang, "Interference avoidance mechanisms in the hybrid cellular and device-to-device systems," *in Proc. IEEE PIMRC, 2009, pp. 617-621*, 2008.

[14] G. Fodor, E. Dahlman, G. Mildh, S. Parkvall, N. Reider, G. Miklós, and Z. Turányi, "Design aspects of network assisted device-to-device communications," *IEEE Communications Magazine*, vol. 50, no. 3, 2012.

[15] J. C. Li, M. Lei, and F. Gao, "Device-to-device (d2d) communication in mu-mimo cellular networks," in *Global Communications Conference (GLOBECOM), 2012 IEEE*. IEEE, 2012, pp. 3583–3587.

[16] "3GPP TS 23.303, proximity-based services (prose); stage 2 (release 12), v.12.0.0," February 2014.

[17] "3GPP TR 36.843 feasibility study on LTE device to device proximity services - radio aspects," 2014.

[18] "3GPP TS 36.213, E-UTRA physical layer procedures."

[19] P. Phunchongharn, E. Hossain, and D. Kim, "Resource allocation for device-to-device communications underlaying LTE-advanced networks," *IEEE Wireless Communications*, vol. 20, no. 4, pp. 91–100, 2013.

[20] C. Yu, O. Tirkkonen, K. Doppler, and C. Ribeiro, "On the performance of device-to-device underlay communication with simple power control," in *IEEE 69th Vehicular Technology Conference*, 2009, pp. 1–5.

[21] Y. Wen-Bin, M. Souryal, and D. Griffith, "LTE uplink performance with interference from in-band device-to-device (D2D) communications," in *IEEE Wireless Communications and Networking Conference*, March 2015, pp. 669–674.

[22] H. Baya, A. Essa, T. Tuytelaars, and L. V. Gool, "Speeded-up robust features (surf)," *Computer Vision and Image Understanding, Volume 110, Issue 3, June 2008, Pages 346-359*, June 2008.
[23] Z. Zivkovic, "Improved adaptive gaussian mixture model for background subtraction," in *Pattern Recognition, 2004. ICPR 2004. Proceedings of the 17th International Conference on*, vol. 2. IEEE, 2004, pp. 28–31.
[24] F. Bashir and F. Porikli, "Performance evaluation of object detection and tracking systems," *Proceedings 9th IEEE International Workshop on PETS. 2006*, 2006.
[25] C. J. Watkins and P. Dayan, "Q-learning," *Machine learning*, vol. 8, no. 3-4, pp. 279–292, 1992.
[26] S. Baidya and M. Levorato, "Content-based Interference Management for Video Transmission in D2D Communications Underlaying LTE," *IEEE International Conference on Computing, Networking and Communication (ICNC) 2017*, 2017.
[27] "NS-3 open source network simulator under GNU GPLv2 license," *https://www.nsnam.org/*.
[28] L. Badia, M. Levorato, and M. Zorzi, "Analysis of selective retransmission techniques for differentially encoded data," *IEEE International Conference on Communications - ICC*, 2009.
[29] A. Asadi, Q. Wang, and V. Mancuso, "A survey on device-to-device communication in cellular networks," *IEEE Communications Surveys & Tutorials*, vol. 16, no. 4, pp. 1801–1819, 2014.
[30] J. Liu, N. Kato, J. Ma, and N. Kadowaki, "Device-to-device communication in lte-advanced networks: A survey," *IEEE Communications Surveys & Tutorials*, vol. 17, no. 4, pp. 1923–1940, 2015.
[31] P. Cheng, L. Deng, H. Yu, Y. Xu, and H. Wang, "Resource allocation for cognitive networks with d2d communication: An evolutionary approach," in *Wireless Communications and Networking Conference (WCNC), 2012 IEEE*. IEEE, 2012, pp. 2671–2676.
[32] Y. Zhao, M. Song, and C. Xin, "Fmac: A fair mac protocol for coexisting cognitive radio networks," in *INFOCOM, 2013 Proceedings IEEE*. IEEE, 2013, pp. 1474–1482.
[33] K. Doppler, C.-H. Yu, C. B. Ribeiro, and P. Janis, "Mode selection for device-to-device communication underlaying an lte-advanced network," in *Wireless Communications and Networking Conference (WCNC), 2010 IEEE*. IEEE, 2010, pp. 1–6.
[34] Z. Liu, T. Peng, S. Xiang, and W. Wang, "Mode selection for device-to-device (d2d) communication under lte-advanced networks," in *Communications (ICC), 2012 IEEE International Conference on*. IEEE, 2012, pp. 5563–5567.
[35] G. Fodor and N. Reider, "A distributed power control scheme for cellular network assisted d2d communications," in *Global Telecommunications Conference (GLOBECOM 2011), 2011 IEEE*. IEEE, 2011, pp. 1–6.
[36] A. Babaei, J. Andreoli-Fang, Y. Pang, and B. Hamzeh, "On the impact of lte-u on wi-fi performance," *International Journal of Wireless Information Networks*, vol. 22, no. 4, pp. 336–344, 2015.
[37] "Extending lte advanced to unlicensed spectrum," *Qualcomm Incorporated, White Paper, December 2013*.
[38] J. Jeon, H. Niu, Q. Li, A. Papathanassiou, and G. Wu, "Lte with listen-before-talk in unlicensed spectrum," *In 2015 IEEE International Conference on Communication Workshop (ICCW), pp. 2320-2324*, 2015.
[39] E. Almeida, A. Cavalcante, R. Paiva, F. Chaves, F. Abinader, R. Vieira, S. Choudhury, E. Tuomaala, and K. Doppler, "Enabling LTE/WiFi coexistence by LTE blank subframe allocation," *in Proc. 2013 IEEE International Conference on Communications (ICC '13), Budapest, Hungary, pp.5083-5088*, 2013.
[40] T. C. Thang, H. T. Le, A. T. Pham, and Y. M. Ro, "An evaluation of bitrate adaptation methods for http live streaming," *IEEE Journal on Selected Areas in Communications*, vol. 32, no. 4, pp. 693–705, 2014.
[41] T. C. Thang, Q.-D. Ho, J. W. Kang, and A. T. Pham, "Adaptive streaming of audiovisual content using mpeg dash," *IEEE Transactions on Consumer Electronics*, vol. 58, no. 1, 2012.
[42] F. Fitzek and M. Reisslein, "Mpeg-4 and h. 263 video traces for network performance evaluation," *IEEE Network*, vol. 15, no. 6, pp. 40–54, 2001.
[43] M. Bramberger, J. Brunner, B. Rinner, and H. Schwabach, "Real-time video analysis on an embedded smart camera for traffic surveillance," in *10th IEEE Real-Time and Embedded Technology and Applications Symposium*. IEEE, 2004, pp. 174–181.
[44] S. Baidya and M. Levorato, "Edge-assisted computation-driven dynamic network selection for real-time services in the urban iot," in *IEEE International Workshop on Advances in Software Defined and Context Aware Cognitive Radio Networks (IEEE SCAN-2017)*.

Sabur Baidya received the B.S. degree in Electronics and Communication Engineering from the WBUT, India, and M.S. degree in Computer Science from the University of Texas at Dallas, TX, USA, in 2007 and 2013, respectively. He is currently pursuing the Ph.D. degree in the Department of Computer Science at University of California, Irvine, CA, USA. He has had prior working and internship assignments in IBM, Cisco, Huawei Research Lab and Nokia Bell Labs. His research interests include Wireless and Cognitive Networks, Internet of Things, Software Defined Networking, Edge Computing and UAVs.

Marco Levorato joined the Computer Science department at University of California, Irvine in August 2013. Between 2010 and 2012, He was a post-doctoral researcher with a joint affiliation at Stanford and the University of Southern California working with prof. Andrea Goldsmith and prof. Urbashi Mitra. From January to August 2013, he was an Access post-doctoral affiliate at the Access center, Royal Institute of Technology, Stockholm. He is a member of the ACM, IEEE and IEEE Comsoc society. His research interests are focused on next-generation wireless networks, signal processing, cyber-physical systems, smart city and smart energy systems. He has co-authored over 75 technical articles on these topics, including the paper that has received the best paper award at IEEE GLOBECOM (2012). He completed the PhD in Electrical Engineering at the University of Padova, Italy, in 2009. He obtained the B.S. and M.S. in Electrical Engineering summa cum laude at the University of Ferrara, Italy in 2005 and 2003, respectively. In 2016, he received the UC Hellman Foundation Award for his research on Smart City IoT infrastructures.